Cross-Bridge Duty Cycle in Isometric Contraction of Skeletal Myofibrils[†]

P. Muthu, J. M. Talent, I. Gryczynski, and J. Borejdo*

Department of Molecular Biology & Immunology and Center for Commercialization of Fluorescence Technology, the University of North Texas HSC, Fort Worth, Texas 76107

Received November 23, 2007; Revised Manuscript Received February 19, 2008

ABSTRACT: During interaction of actin with myosin, cross-bridges impart mechanical impulses to thin filaments resulting in rotations of actin monomers. Impulses are delivered on the average every t_c seconds. A cross-bridge spends a fraction of this time (t_s) strongly attached to actin, during which it generates force. The "duty cycle" (DC), defined as the fraction of the total cross-bridge cycle that myosin spends attached to actin in a force generating state (t_s/t_c), is small for cross-bridges acting against zero load, like freely shortening muscle, and increases as the load rises. Here we report, for the first time, an attempt to measure DC of a single cross-bridge in muscle. A single actin molecule in a half-sarcomere was labeled with fluorescent phalloidin. Its orientation was measured by monitoring intensity of the polarized TIRF images. Actin changed orientation when a cross-bridge bound to it. During isometric contraction, but not during rigor, actin orientation oscillated between two values, corresponding to the actin-bound and actin-free state of the cross-bridge. The average t_s and t_c were 3.4 and 6 s, respectively. These results suggest that, in isometrically working muscle, cross-bridges spend about half of the cycle time attached to actin. The fact that $1/t_c$ was much smaller than the ATPase rate suggests that the bulk of the energy of ATP hydrolysis is used for purposes other than performance of mechanical work.

From the analysis of crystal structures of different forms of myosin, single-molecule studies, spectroscopic experiments, and X-ray diffraction of muscle fibers, a picture of the cross-bridge cycle emerges that suggests that during muscle contraction a cross-bridge assumes at least two distinct conformations: strongly attached to actin and dissociated from it (*1*−*3*). It is believed that a strongly attached cross-bridge produces contractile force. Cross-bridge is in a strongly attached state for a period of time t_s, after which the contractile cycle continues with a release of phosphate followed by the dissociation of ADP and the onset of rigor. Its end is marked by the binding of a fresh molecule of ATP and detachment of myosin from actin. Finally, ATP is hydrolyzed to ADP and phosphate, and the cycle repeats with the period t_c. In this scheme, the motion of switch I (a loop in the upper 50K domain of S1) is coupled to the actin-binding cleft, and the motion of switch II (the loop which contains invariant glycine that forms a hydrogen bond with γ-phosphate of ATP) is coupled to the lever arm. The opening of switch I provides an exit route for P_i. The power stroke is initiated by actin binding to a myosin that contains hydrolysis products, via closure of the 50 kDa cleft. This is followed by opening of switch I, thereby reducing its interactions with switch II. This allows switch II to open. It is possible that the power stroke occurs in two steps: the initial generation of force associated with the weak to strong transition of actomyosin (containing products of hydrolysis). This leads to the rotation of the whole myosin head before the internal structural change of switch II occurs. The motion of the head is followed by the swing of the lever arm that is associated with P_i release (*4*).

In vitro evidence, based on observation of the individual steps of skeletal actin (*5*), smooth myosin (*6, 7*) and myosin V (*8*−*10*), suggests that the duty cycle DC,[1] defined as the ratio of t_s/t_c, is small for cross-bridges acting against zero load (*5, 11, 12*). Here we report the attempt to measure DC of a single cross-bridge in muscle. We were motivated by realization that DC could be measured directly if the individual impulses could be visualized during isometric contraction. Individual impulses can only be visualized if single molecules were observed. Observation of individual molecules in a tissue is not a simple matter, especially in muscle where the concentration of protein is very large (*13*). The observation of a single molecule in muscle is reported here for the first time.

To illustrate how important it is to know the DC, consider a consequence of assuming that DC in isometric contraction is low (say 0.05). This is the value determined for a single myosin molecule in vitro (*14, 15*). An even lower value (DC = 0.031) was calculated by Mitsui (*16*) from X-ray results of Watanabe (*17*). The value of DC is calculated as the ratio of maximal isometric tension (P) to tension developed by one cross-bridge (p), normalized by the number of cross-bridges in a cross-section of muscle (N), DC = $P/(pN)$ or p

[†] Supported by NIH Grant R01AR048622 to J.B. and by Texas ETF grant (CCFT).

* Corresponding author: Julian Borejdo, Department of Molecular Biology, University of North Texas Health Science Center, 3500 Camp Bowie Blvd, Fort Worth, TX 76107. Tel.: 817 735-2106. Fax: 817 735 2118. E-mail: jborejdo@hsc.unt.edu.

[1] Abbreviations: DC, duty cycle of the cross-bridge; VM, video measurements; CTIR, confocal total internal reflection; SMD, single molecule detection; S/N, signal-to-noise; RP, rhodamine phalloidin; UP, unlabeled phalloidin; EDC, 1-ethyl-3-(3′-dimethylaminopropyl) carbodiimide; ROI, region-of-interest; DTT, Cleland's reagent.

10.1021/bi7023223 CCC: $40.75
Published on Web 04/22/2008

$= P/[(DC)N]$. Taking isometric tension as $4.1 \times 10^5 N/m^2$ (*18*) and the number of myosin heads in one half-sarcomere 1.76×10^{17} in 1 m^{-2} cross-section of muscle (*19*) gives $p = 47$ pN. This is 8 times larger than the value determined experimentally (5.7 pN) (*20*). It also implies that the step size is 30 nm, whereas reported value is 10 nm (*21*). The value of DC which would have been consistent with measured P and p is DC = 0.41. This value is close to the one determined experimentally by stiffness measurements (*22*). An intermediate value was obtained by Cooke et al. (*23*) using electron spin resonance data. They observed that only 20% of the spin labeled myosin were bound to actin in isometrically contracting muscle. Similar results were obtained by Duong and Reisler (*24*), who showed that 25% of the myosin heads in calcium activated EDC-cross-linked myofibrils (not modified at SH1) were protected from tryptic digestion at the 50/20 kDa junction in the myosin heavy chain. Berger and Thomas (*25*) confirmed these results and showed that this value increased to 37% at low ionic strength, presumably due to additional contributions from weakly bound cross-bridges. Berger and his collaborators estimated that close to 1/3 cross-bridges are active during isometric contraction (*26*). Thus, experiments that can directly measure the actomyosin interaction of a single cross-bridge under isometric conditions within the myofilament lattice are clearly needed to resolve these important issues.

In a strongly bound state the rotational freedom of a cross-bridge is inhibited as demonstrated by the high anisotropy of cross-bridges in rigor (*27*). In a dissociated state, the rotational freedom is restored, as demonstrated by the low anisotropy of relaxed muscle (*27, 28*). The same changes of anisotropy are observed in actin (*29*). Observing actin has a number of essential advantages that make study of single molecules in muscle possible. First, actin can be labeled specifically and stoichiometrically with fluorescent phalloidin, which allows strict control of the degree of labeling. Second, labeling with phalloidin has the advantage that, in skeletal muscle (in contrast to cardiac muscle), only the ends of thin filaments are initially labeled (*30*). This is the region (overlap zone, O-band) where actin and cross-bridges interact. Third, phalloidin does not alter enzymatic properties of muscle (*31, 32*) and does not impair the regular structure of a myofibril, like the less gentle labeling of myosin does.

Actin was labeled with a 10^5:1 mixture of nonfluorescent: fluorescent phalloidin, assuring that on average less than one molecule of actin per half-sarcomere was fluorescent. The orientation was measured by monitoring intensities of the polarized TIRF images of half-sarcomere that contained no more than 3 actin molecules. Polarization could be measured because fluorescent phalloidin was partly immobilized by actin filaments. The polarized intensity closely followed polarization of fluorescence, which is an established probe of the orientation (*33*). During isometric contraction, but not during rigor, actin orientation oscillated between two values, corresponding to the actin-bound and actin-free state of the cross-bridge. The average cycle time t_c was 6 s. The cross-bridge stayed attached to actin on average $t_s = 3.4$ s. These results suggest that in isometrically working muscle cross-bridges spend about half of cycle time attached to actin, and that the bulk of the energy of ATP hydrolysis is used for purposes other than performance of mechanical work.

MATERIALS AND METHODS

Chemicals and Solutions. Rhodamine phalloidin (RP) was from Molecular Probes (Eugene, OR). Unlabeled phalloidin (UP) was from Sigma (St Louis, MO). All other chemicals including 1-ethyl-3-(3′-dimethylaminopropyl) carbodiimide (EDC), phosphocreatine, creatine kinase, glucose oxidase, catalase and ATP were from Sigma. EDTA-rigor solution contained 50 mM KCl, 2 mM EDTA, 1 mM DTT, 10 mM Tris-HCl buffer pH 7.5. Ca-rigor solution contained 50 mM KCl, 4 mM $MgCl_2$, 0.1 mM $CaCl_2$, 1 mM DTT, 10 mM Tris-HCl buffer pH 7.5. Mg-rigor solution contained 50 mM KCl, 4 mM $MgCl_2$, 1 mM DTT, 10 mM Tris-HCl buffer pH 7.5. Contracting solution was the same as Ca-rigor, except that it contained in addition 2 mM ATP.

Sample Cross-Linking. Muscle was washed with cold EDTA-rigor solution for $1^1/_2$ h followed by an extensive wash with Mg-rigor, followed by washing with Ca-rigor solution. Myofibrils were made from muscle in Ca-rigor as described before (*28*). In order to prevent shortening during contraction, myofibrils were lightly cross-linked with water-soluble cross-linker EDC (*34*). Myofibrils (1 mg/mL) were incubated with 2 mM EDC for 10 min at room temperature. The reaction was stopped by 20 mM DTT. The lack of shortening was checked under differential contrast (*35*). In 8 control experiments, the mean ± SD sarcomere length of rigor and contracting myofibrils remained unchanged from 2.77 μm ± 0.14 μm in rigor to 2.78 μm ± 0.12 μm during contraction. The paired t test showed that the difference was not statistically significant ($t = 0.42$, $P = 0.68$, 8 degrees of freedom). It has been shown that cross-liked myofibrils were a good in vitro model for muscle fiber ATPase and the kinetics of Ca(2+)-activated activity (*36*). The large $P(i)$ bursts and k_{cat} values were also the same in cross-linked myofibrils and muscle fibers (*34*). Those results were confirmed by Lionne et al. (*37*).

Labeling and Sample Preparation. Myofibrils (1 mg/mL) were labeled for 5 min with a mixture containing 0.1 nM RP + 10 μM UP in Ca-rigor solution. If unlabeled phalloidin was not included, the number of fluorophores in a half-sarcomere would depend on the way fluorescent phalloidin was mixed with myofibrils. Labeled myofibrils (25 μL) were applied to 20 mm diameter sapphire coverslips (Olympus; precleaned with 100% ethanol). A narrow channel was created by applying a thin layer of petroleum jelly along the edges of the coverslip. To align myofibrils as much as possible along the long axis of a coverslip, the sample was applied by streaking the pipet along the long axis. The sample was left on a coverslip for 3 min to allow myofibrils to adhere to the sapphire. The sapphire coverslip was covered with a small (5 mm diameter) glass coverslip and washed with at least 5 volumes of Ca-rigor solution by applying the solution to one end of the channel and absorbing with #1 filter paper at the other end.

Imaging. The instrument was described before (*35, 38*). In the present experiments, the Hamamatsu ImagEM CCD camera (Hamamatsu, Bridgewater, NJ) was mounted in the right exit port (model IX2 RSPC-2) of the microscope. The left exit port contained a confocal aperture and the Avalanche Photodiode, as previously described (*35*), to measure the num-

ber of photons emitted by muscle.[2] Excitation light from an expanded DPSS laser beam (Compass 215M, Coherent, Santa Clara, CA) was projected by a polarization-preserving-fiber to a commercial TIRF attachment (Olympus) and high NA objective (Olympus ×100 NA = 1.65 or ×60 NA = 1.45). The totally internally reflected light produced an evanescent wave on the aqueous side of the interface (*39*). The sample rested on a movable piezo stage (Nano-H100, Mad City Laboratories, Madison, WI) controlled by a Nano-Drive. The fluorescent light was collected through the same objective, projected onto a tube lens and to a calcite prism (Melles Griot, Carlsbad, CA) which split the fluorescent light into two orthogonally polarized components. The light was focused on the photosensitive area of the camera. The insertion of the calcite prism did alter by a few millimeters the position of the conjugate image plane, but it made a negligible difference to the focus because the high magnification objective (with long back focal distance) was used. All experiments were done at room temperature.

Spatial Sampling. The pixel size of the camera is 16 μm ×16 μm. For the 100× NA 1.65 objective with 532 nm illumination, the Rayleigh resolution limit is ∼200 nm. According to the Nyquist sampling theorem, the ideal spatial sampling rate should have been 200/2.3 ≈ 90 nm. The back-projected size of the pixel of the camera is 16 μm/100 = 160 nm. Therefore the images are undersampled by a factor of 160/ 90 ≈ 1.8. For the 60× NA 1.45 objective, the back-projected size of the pixel of the camera is 267 nm and the images are undersampled by a factor of ∼3. Undersampling allows the light to be concentrated on fewer pixels. Under the present low-light conditions, this creates a signal that has greater amplitude relative to the background noise, and therefore boosts signal-to-noise (S/N) ratio.

Temporal Sampling. The whole field (512 × 512 pixels) was collected at time intervals τ. The choice of τ is crucial in single molecule detection (SMD). Decreasing τ increases time resolution but decreases the number of fluorescent photons detected from each half-sarcomere. Increasing τ improves S/N ratio but decreases time resolution. We used τ = 200 ms, a reasonable compromise since the characteristic time for ATP hydrolysis by glycerinated skeletal myofibrils is in the 0.5−2 s range (*40*). Five hundred (500) images (100 s) of data were collected.

Image Analysis. HCImage software (Hamamatsu) was used. In a 512 × 512 image, a 4 × 4 pixel rectangular region-of-interest (ROI) was created containing one O-band. The intensity measurement tool was used to measure mean gray value of all the defined ROIs in all 500 images. This data was saved as tabbed text file. The ASCII file was plotted in SigmaPlot (Systat, San Jose, CA).

Anisotropy and Lifetime Measurements. Fluorescence lifetimes and anisotropies were measured by time-domain technique using FluoTime 200 fluorometer (PicoQuant, Inc.).

[2] In principle it is possible to calculate number of photons from the gray level of the camera using the following formula: number of photons/pixel = [gray level × conversion efficiency]/[gain × quantum efficiency]. Conversion and quantum efficiencies for Hamamatsu ImagEM CCD camera are 5.07 e^-/pixel and 0.9 (at 700 nm), respectively. But it is extremely difficult to determine the gain, which depends very critically on temperature. Each EM CCD chip has a gain vs temperature curve which is very nonlinear. Experimental determination of the number of photons, as outlined here, seems the best approach.

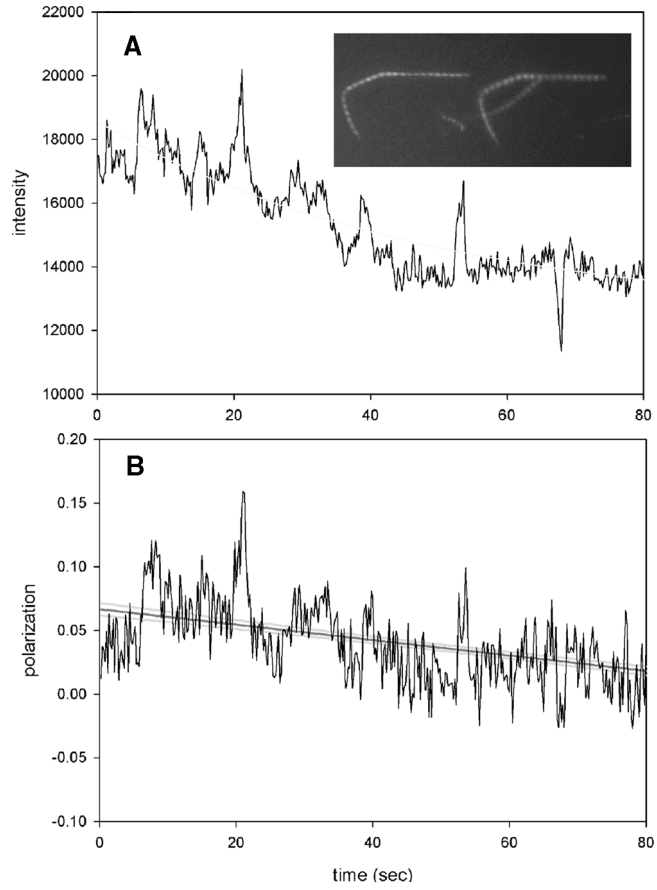

FIGURE 1: Comparison of polarized intensities and polarization of fluorescence. (A) Horizontal polarized intensity. Inset shows the two orthogonally polarized images: left, emitted light polarized parallel to the myofibrillar axis; right, emitted light polarized perpendicular to the myofibrillar axis. Exciting light polarized horizontally. White line is 3 parameter exponential function showing poor fit to the data. (B) Polarization of fluorescence. Myofibril labeled with 1 nM RP + 10 μM UP. Thick line is the best linear fit; gray lines indicate 95% confidence limit.

The excitation was by a 475 nm laser pulsed diode, and the observation was through a monochromator at 575 nm with a supporting 550 nm long wave pass filter. The fwhm of the pulse response function was 68 ps (measured by PicoQuant, Inc.). The time resolution was better than 10 ps. The intensity decays were analyzed in terms of a multiexponential model using FluoFit software (PicoQuant, Inc.).

RESULTS

Polarized Intensity Is a Good Measure of Orientation. The established measures of orientation are polarization of fluorescence (P) or anisotropy (A) defined as $P = (I_{||} - I_{\perp})/(I_{||} + I_{\perp})$ and $R = (I_{||} - I_{\perp})/(I_{||} + 2I_{\perp})$ where $I_{||}$ and $I_{\perp}$ are the fluorescence intensities of the vertically (||) or horizontallly ($\perp$) polarized emission when the sample is excited with vertically polarized light (*33*). In the present experiment, however, we found it convenient to measure only $I_{||}$, because P and R are noisy due to division of two noisy signals. Moreover, the noise of P or R measurements is increased because regions-of-interest placed over corresponding orthogonally polarized sarcomeres are often slightly out of register. It is therefore essential to demonstrate that $I_{||}$ behaves like P or R. The inset to Figure 1A shows two orthogonal images of a myofibril. Figure 1 compares the time course of

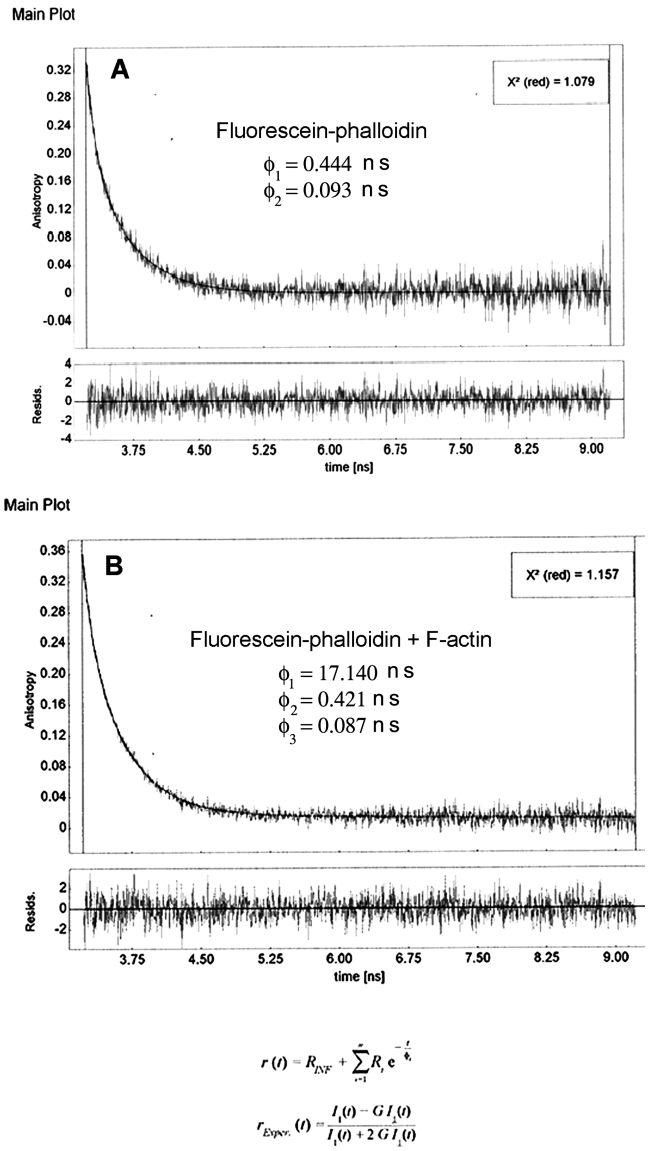

$$r(t) = R_{INF} + \sum_{i=1}^{n} R_i e^{-\frac{t}{\phi_i}}$$

$$r_{Exper.}(t) = \frac{I_{\parallel}(t) - G I_{\perp}(t)}{I_{\parallel}(t) + 2 G I_{\perp}(t)}$$

FIGURE 2: Decay of anisotropy of fluorescein phalloidin (A) and fluorescein phalloidin bond to F-actin (B). Binding of phalloidin to F-actin results in a significant immobilization of the probe. (A) 0.1 μM fluorescein phalloidin, (B) 2 μM F-actin containing 0.5 μM fluorescein phalloidin. The equation shows the model to which anisotropy was fitted. R_{INF} was fixed at 0.

horizontal intensity (A) with parallel polarization of fluorescence (B) defined as $[(I_{left} - I_{bckl}) - (I_{right} - I_{bckr})]/[(I_{left} - I_{bckl}) + (I_{right} - I_{bckr})]$ where I_{left} and I_{right} are the intensities of the corresponding half-sarcomeres in the left and right images, respectively, and I_{bckl} and I_{bckr} are the intensities of the left and right background immediately adjacent to a myofibril. It is seen that horizontally polarized intensity closely follows the polarization of fluorescence signal and is therefore a good measure of orientation.

For quantitative measurement of orientation, one needs to know whether the probe is at least partially immobilized by the protein so that the transition dipole of the fluorophore reflects the orientation of the protein. Figure 2 shows that this is the case for fluorescent phalloidin labeling F-actin. The decay of anisotropy of fluorescein phalloidin is shown in Figure 2A. 93% and 7% of the signal was contributed by the decay times of 0.444 and 0.093 ns, respectively. The longer correlation time is due to the rotation of phalloidin, and the shorter one to the independent rotation of fluorescein moiety. Thus the free rotation of fluorophore contributes negligibly to the signal. Figure 2B shows the decay of anisotropy of fluorescein phalloidin coupled to F-actin. 28%, 69% and 3% of the signal was contributed by the decay times of 17.140, 0.421 and 0.087 nsec, respectively. The longest correlation time is due to the rotation of F-actin oligomers, intermediate one to the rotation of phalloidin, and the shortest one to the independent rotation of fluorescein moiety. Thus a significant fraction of fluorescent phalloidin is immobilized by F-actin, and therefore contributes to the anisotropy of muscle (nonimmobilized phalloidin does not, because it rotates rapidly on the time scale of the measurement).

The fluorescent lifetime of phalloidin could be best fitted by three exponentials with lifetimes of 3.471, 1.708 and 0.044 ns and relative contributions of 63%, 33% and 4%, respectively. The amplitude weighted lifetime was 2.156 ns. Binding to F-actin changed lifetimes by less than 1%.

Concentration of Fluorophores Needed To Observe a Single Molecule in Muscle. To establish conditions necessary to observe a single molecule of actin in muscle, we followed the course of photobleaching of a half-sarcomere containing actin labeled with fluorescent phalloidin. We first demonstrate that if the number of fluorophores is large enough, photobleaching occurs with the expected exponential time course. We reasoned that ~100−500 fluorophores in a half-sarcomere would be needed to ensure smooth decay of fluorescence. The typical height, width and length of a sarcomere are 0.1 μm, 0.8 μm and 2.5 μm, respectively (*41*), so its volume is 0.2 $\mu m^3 = 0.2 \times 10^{-15}$ L. Since the concentration of actin in muscle is 0.6 mM (*13*), this volume contains 0.7×10^5 actin monomers. Therefore to ensure that ~1 in 10^2 molecules are labeled, we have to label with 100 nM RP (+9.9 μM nonfluorescent label), i.e. fix the ratio of fluorescent to nonfluorescent phalloidin as 1:100. The top panel of Figure 3 shows the time course of photobleaching of the myofibrils labeled with 100 nM RP + 9.9 μM UP. The images were captured every 200 ms; only the first, 10th, 50th, 100th, 200th, 300th and 500th frames are shown. The time course of photobleaching of the O-band (spot number 29 in the entire image) pointed to by the arrow in the top panel is plotted in gray in the left bottom panel of Figure 3. Photobleaching of the adjacent background area (spot number 19) of the same size (4×4 pixels) pointed to by the arrowhead in the top panel is plotted in black. This signal probably originates from fluorophores that are washed out from the muscle and become stuck to the coverslip. The difference between the two is plotted in the right bottom panel. As expected, the time course of photobleaching is smooth. The fit to the three parameter exponential (shown in white) $y = 2806 + 11577e^{-4.4\times10^{-3}t}$ is good. The half-time is ~40 s.

Single Molecule Measurements. On the basis of this experiment, we estimate that in order to see individual molecules we need a 1000-fold smaller concentration of phalloidin.

The top panel of Figure 4 shows the time course of photobleaching of contracting myofibril labeled with 0.1 nM RP + 10 μM UP. Only the first, 10th, 50th, 100th, 200th, 300th, 400th and 500th frames are shown. The time course of photobleaching of the O-band pointed to by the arrow in the top panel is plotted in the left middle panel (gray). The time course of photobleaching of the 4×4 pixel background immediately adjacent to the analyzed O-band, pointed to by

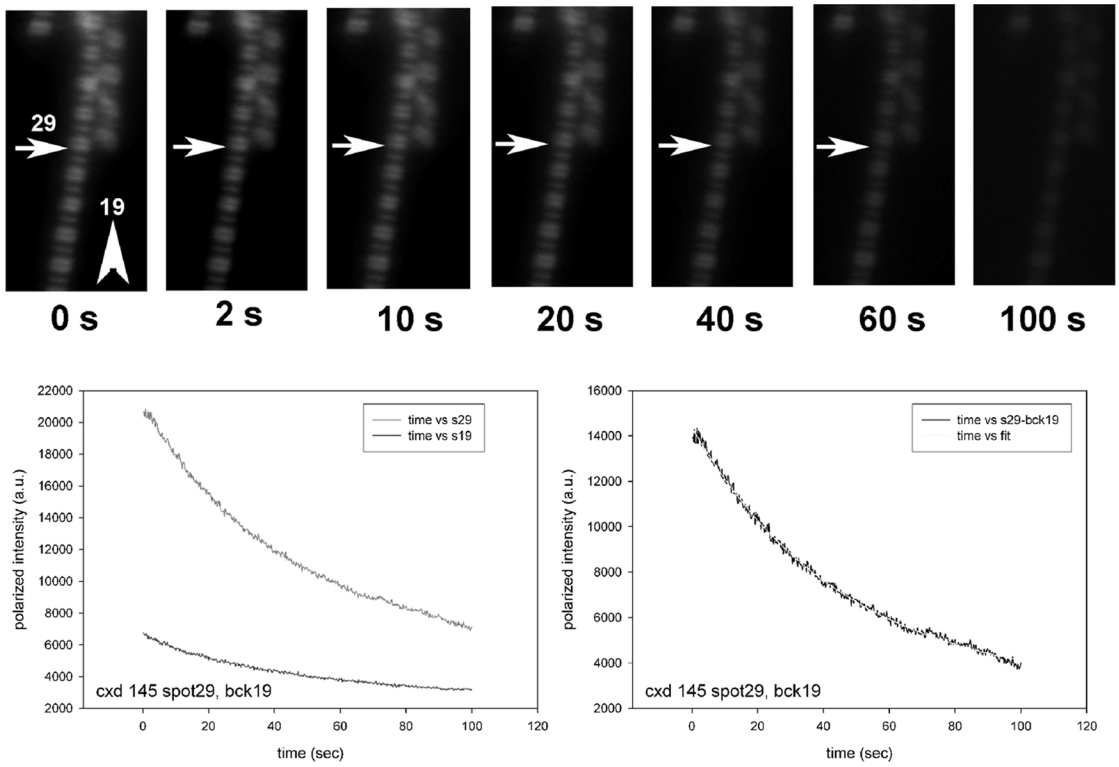

FIGURE 3: The time course of photobleaching of heavily labeled rigor myofibril. Top panel: Polarized images of a myofibril at times indicated below each frame ($s = 1$ s). Exciting light is polarized vertically, emitted light polarized horizontally with respect to the myofibrillar axis. Bottom left panel: The time course of photobleaching of the O-band pointed to by the arrow in the top panel (gray). The time course of photobleaching of 4 × 4 pixel background pointed to by the arrowhead in the top panel (black). Bottom right panel: The time course after background subtraction. The least-squares 3-parameter exponential fit (white) is $y = 2806 + 11577e^{-4.4\times10^{-3}t}$. Myofibril is labeled with 100 nM RP + 9.9 μM UP. Myofibrils are on sapphire coverslip, viewed by 100× NA = 1.65 objective.

the arrowhead in the top panel, is plotted in black. The time course of photobleaching of the difference between the intensity of the O-band and adjacent background is plotted in the right middle panel of Figure 4. In this case we observed 3 molecules, because photobleaching occurred in three steps. The stepwise decrease in signal is visible even though the 3 fluorophores are most likely localized at different distances from the surface of the coverslip, and therefore bleach with different efficiencies.

Fluctuations in orientation of actin in the O-band are greater before than after photobleaching step. The power in the first 20 s part of the signal (before photobleaching) is shown in the bottom panel of Figure 4 in black. The power in the last 20 s part of the signal (after photobleaching) is shown in the bottom panel of Figure 4 in gray. On numerous occasions, there was only a single fluorophore in the O-band. A typical example is shown in Figure 5. The top panel shows the time course of photobleaching of contracting myofibrils labeled with 0.1 nM RP + 10 μM UP. The time course of photobleaching of the O-band pointed to by the arrow in the top panel is plotted in the left middle panel (gray). The time course of photobleaching of the 4 × 4 pixel background pointed to by the arrowhead in the top panel is plotted in black. The time course of photobleaching of the difference between the intensity of the O-band and adjacent background is plotted in the right middle panel of Figure 5 (black). The bottom panel shows the 24 s of head and tail parts of the signal on the expanded time scale (left) and the corresponding power spectra (right).

To analyze fluctuations statistically, the amount of power in the signal before and after the photobleaching event was compared. The signal was divided into two parts: the head part consisting of the signal collected during the beginning of the experiment before the first photobleaching event (containing useful signal + random noise and lasting typically 20−40 s), and the tail part consisting of the signal collected after the second photobleaching step (containing random noise and lasting ~20−40 s). Figure 6 compares the power before and after the photobleaching event in 19 experiments where oscillations were pronounced. In all cases, the peak frequencies of intensity changes were <0.2 Hz. The mean frequency was defined as $\sum fN/\sum N$, where f is a given frequency and N is the number of measurements at this frequency ($\sum N$ is the total number of measurements). The mean frequency was 0.17 Hz, giving mean $t_c \approx 6$ s.

In an attempt to determine t_s, we analyzed in detail 48 experiments as illustrated in Figure 7. The theoretical upper and lower limits were set by the bounds of variation due to random noise $N \pm \sqrt{N}$(mean ± square root of mean). These are drawn as gray lines. It is clear that these limits were rarely exceeded for the background noise (bottom trace). In contracting muscle, on the other hand, the limits were often exceeded (top trace). Actin was judged to contain bound cross-bridge when this limit was exceeded by at least 100%. The arrows indicate full width at half-height (fwhh) of the impulses which satisfied this condition. The histogram of duration of the impulses is plotted in Figure 8. The mean duration, defined as $\sum t_s N/\sum N$, where $t_s$is a given duration and N is the number of measurements with this duration ($\sum N$is the total number of measurements). The mean duration was 3.4 s.

Discrete photobleaching occurred even though the fluorophores were bleaching with different efficiencies. In spite

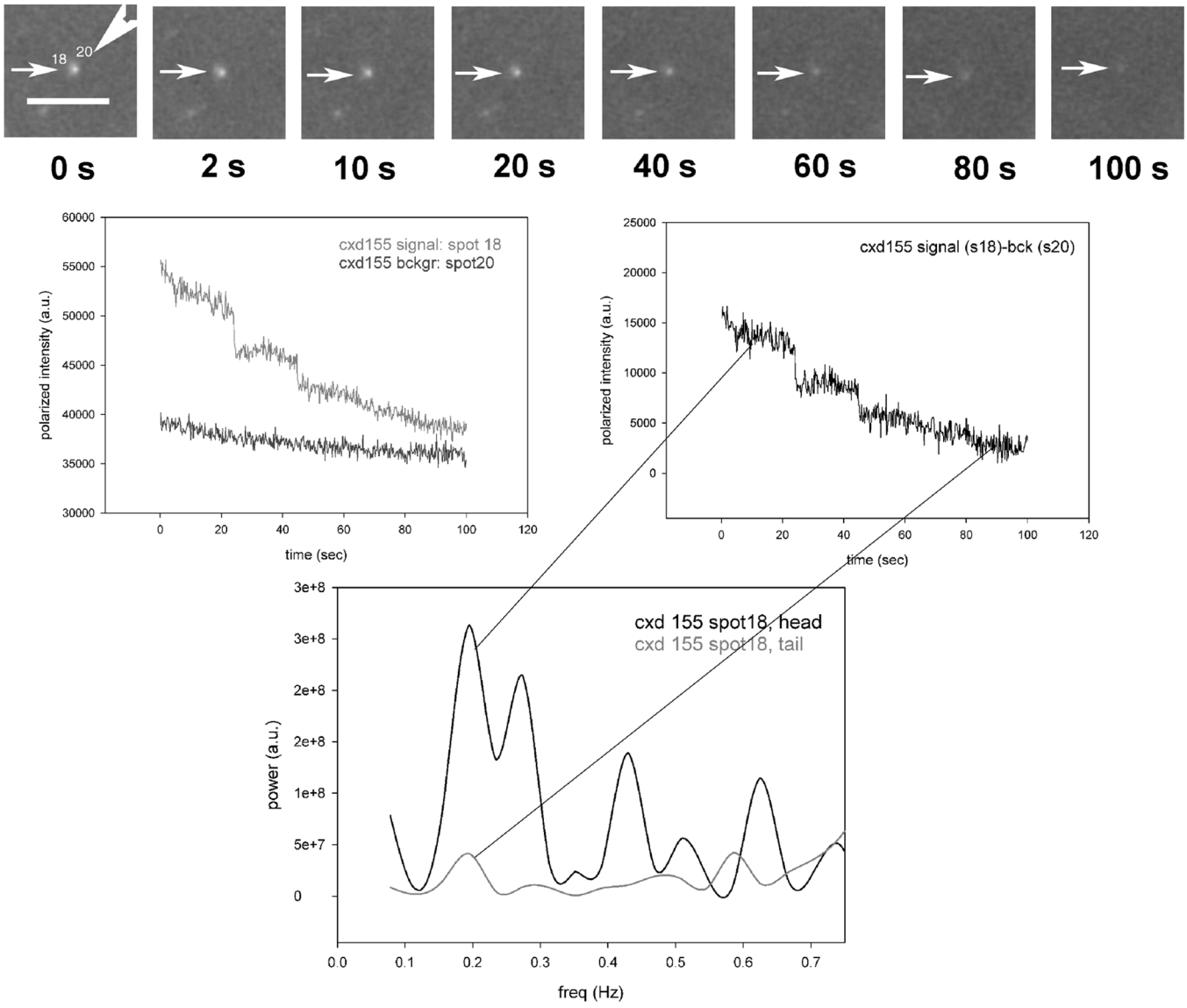

FIGURE 4: The time course of photobleaching of contracting myofibril: 3 fluorophores. Top panels: myofibril at times indicated below each frame ($s = 1$ s). Exciting light is polarized vertically, emitted light polarized horizontally with respect to the myofibrillar axis. The arrows point to the analyzed O-band. The arrowhead points to the 4×4 background pixels. Numbers indicate spot number of the image. The bar is 10 μm. The O-band is ~0.9 μm wide. Middle panel: The time course of photobleaching of the O-band pointed to by the arrow in the top panel. Left: Raw signals from the O-band (gray) and background (black). Bottom panel: Power spectra of the first 20 s (black) and the last 20 s (gray) of the polarized intensity. Myofibril on sapphire coverslip, labeled with 0.1 nM RP + 10 μM UP; viewed with 100×, 1.65 NA objective using 1.78 refractive index immersion liquid.

of this, it was possible to estimate the average duration of a step as ~20 s. Each step led to the decrease of gray level by ~4000. The number of photons corresponding to this gray value was measured by taking advantage of our ability to direct the signal either to the EM CCD camera or to the Avalanche Photodiode (see Materials and Methods). We determined that the gray value drop of 4000 corresponds to a loss of ~800 photons/s. In 20 s we therefore observed ~16,000 photons from a fluorophore before it photobleached. The geometrical collection efficiency of the instrument is ~2% (*35*), thus a fluorophore emitted a total of 0.8×10^6 photons before irreversible bleaching. This is consistent with known photostability of rhodamine (*42*).

Control Experiments. We considered three possible reasons why phalloidin labeling could lead to spurious signal generation. We found them impossible or unlikely: (i) *The signal is not originating from 0.1 nM RP, but from higher concentration of dye because the ON-rate of RP binding is faster than the ON-rate of UP binding.*This is conceivable, in spite of the fact that fluorescent phalloidin is bulkier because it contains an additional rhodamine molecule. The consequence would be that the molar ratio of labeled to unlabeled phalloidin is larger than claimed. The following experiment convinced us that this was unlikely: we have labeled myofibrils with a fixed molar ratio RP:UP of 10^3 and increased by the same factor the absolute concentration of both RP and UP (we used 10 nM, 100 nM and 1 μM of RP and 10 μM, 100 μM and 1 mM of UP). If RP bound faster than UP, more actins would get labeled when higher absolute concentrations were used, and the image would become progressively better. This was not the case. In fact, the image became progressively worse, suggesting that UP binds faster than RP. (ii) *The signal is not originating from 0.1 nM RP, but from higher concentration of the dye because*

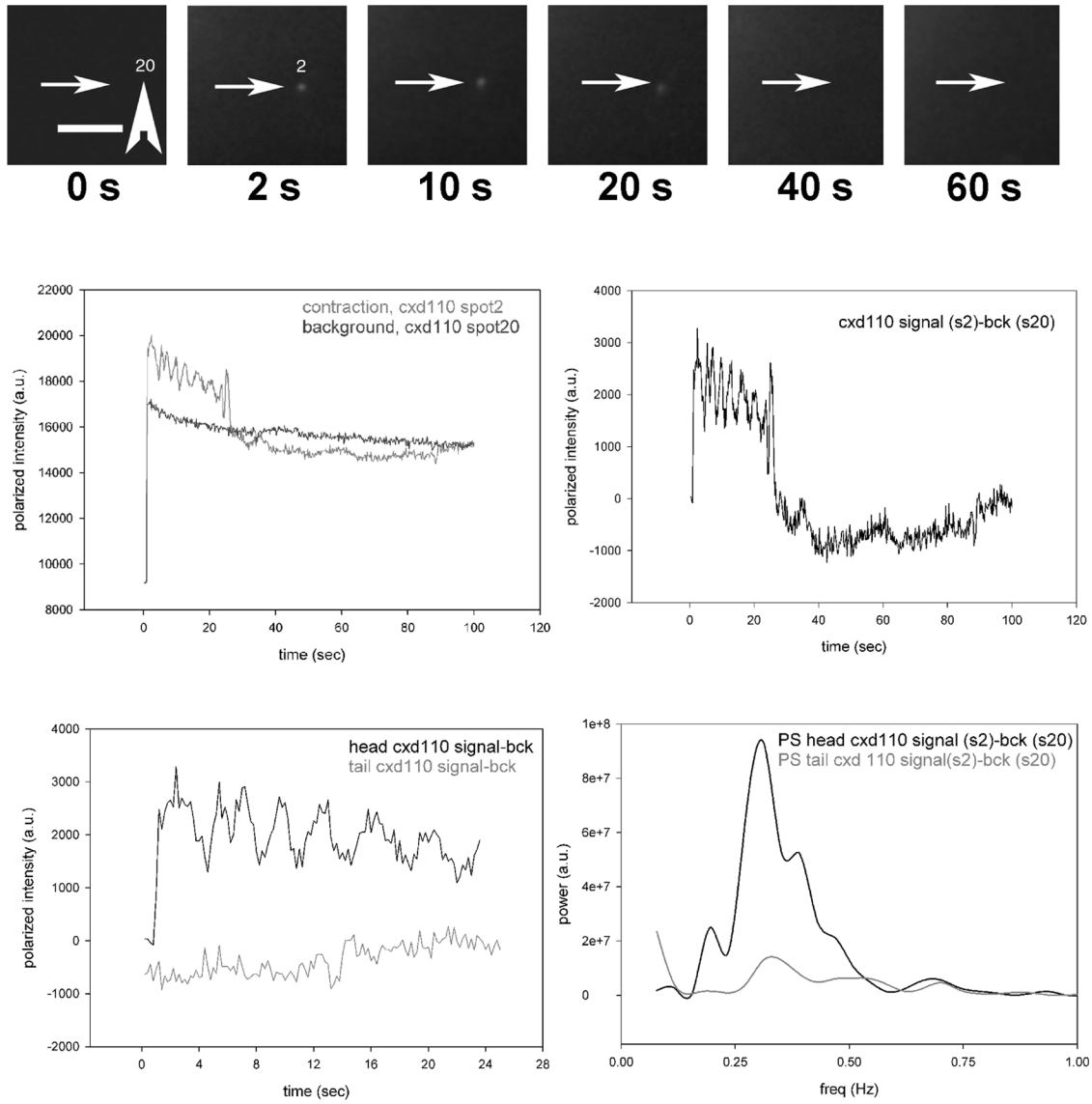

FIGURE 5: The time course of photobleaching of contracting myofibril: single fluorophore. Top panels: Images of contracting O-band. Numbers below each frame indicate the time ($s = 1$ s) after opening the shutter admitting the laser beam. Exciting light is polarized vertically, emitted light polarized vertically with respect to the myofibrillar axis. The bar in the first panel is 10 μm. The O-bandwidth is $\sim$0.8 μm. Arrows point to the O-band analyzed in the bottom panel. Arrowhead points to the background ROI (4 $\times$ 4 pixels). Middle panel: The time course of intensity change of the O-band pointed to by the arrow in the top panel. Gray: absolute intensity. Black: Background pointed to by the arrowhead above. Black in the right panel: the signal-background. Left bottom panel: 24 s of the head (black) and tail (gray) of the signal. Right bottom panel: Power spectra of the head (black) and tail (gray) part of the signal. Myofibrils are labeled with 0.1 nM RP + 10 μM UP.

the OFF-rate of UP is sufficiently fast for RP to displace it from thin filaments. As a consequence, the molar ratio of labeled to unlabeled phalloidin is larger than claimed 1:10[5]. However, this is unlikely because in a control experiment we first labeled 1 mg/mL (4 μM actin) myofibrils with an excess of UP. After brief incubation, we added 4 μM RP in an attempt to displace bound UP with RP. If the OFF-rate of UP were faster than RP, myofibril would have now become fluorescent. This was not the case, suggesting that the off-rate of UP is slow. This is consistent with the fact that the dissociation of phalloidin from actin is known to be slow (4.8×10^{-4} s^{-1} (*43*)), i.e. phalloidin spends on the average 2,000 s on actin before dissociating. (iii) *Fluorescence is due to fluorescent contaminant in unlabeled phalloidin.* This is impossible, because in a control experiment we saturated the myofibrils with 0.6 mM UP and observed no fluorescence whatever.

DISCUSSION

Stepwise Photobleaching. Observation of individual molecules in muscle is complicated by the fact that the concentration of contractile protein is large (*13*) (1 cm long skeletal muscle fiber contains $\sim 10^{13}$ cross-bridges). Even if this number is reduced to a few hundred by the use of confocal (*44*) or two-photon (*45*) microscopy, the averaging makes it impossible to distinguish individual impulses. Recent developments in confocal total internal reflection microscopy (CTIR) allowed observation of actomyosin interactions in a volume small enough to contain only a few molecules (*38*). Muscle was observed on metallic surfaces (*46, 47*) or on glass (*35, 48*). However, those were indirect measurements that relied on autocorrelation of Avalanche Photodiode signals. Here we demonstrated cross-bridge cycle by directly observing orientational state of actin.

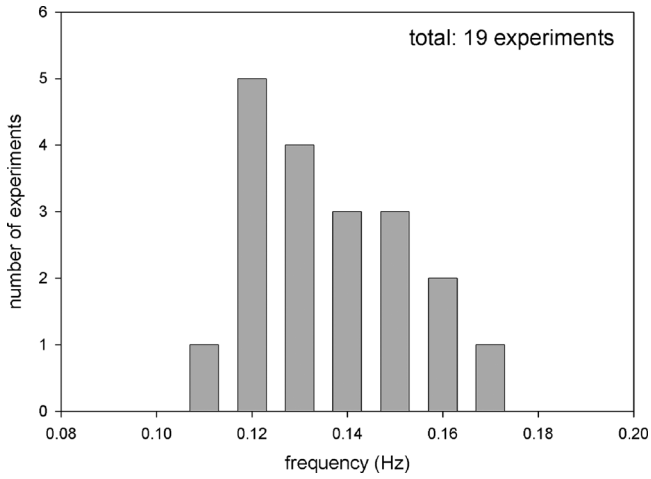

FIGURE 6: Histogram of the peak frequencies of the first 40 s of signals of contracting muscle. The mean frequency is defined as $\sum fN/\sum N$, where f is a given frequency and N is the number of measurements at this frequency. The total number of measurements was 19. The mean frequency was 0.14 ± 0.017 Hz. Analysis does not include experiments in which bleaching occurred in one step. Including these experiments, the average frequency was 0.17 Hz.

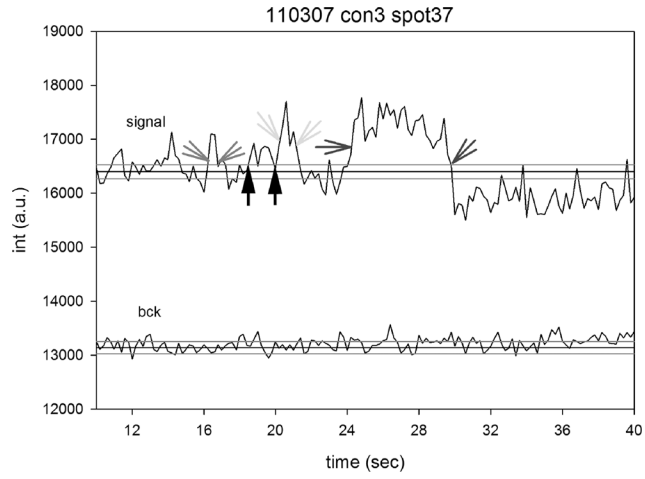

FIGURE 7: Polarized intensity of actin is high when the cross-bridge binds to actin, and low when it detaches from it. The duration of the actin in high state is defined as full width at half-height (fwhh) of the force impulses (indicated by arrows). Top trace: Contracting muscle. Bottom trace: The background. Gray lines indicate the limits of random variation of the noise. Some impulses, such as the one pointed to by the black arrows, were not included in the analysis.

A significant advantage of the present method is that it probes molecules in muscle. It is possible that cross-bridges in functioning muscle behave differently than in solution due to molecular crowding (*49*) and the organization of actin and myosin into regular arrays imposes restrictions on a cross-bridge depending on its position relative to the actin "target site" (*50*).

Measuring t_s. The observed change of actin orientation was similar to the one predicted by the simple model where a cross-bridge is either bound to actin filament or dissociated from it. The average duration of high anisotropy of actin was 3.4 s. We attempted to see if t_s increases with concentation of ATP, like it does in in vitro experiments (*51*) . We carried out 13 experiments using 10 μM ATP to stimulate contraction. The analysis of t_s (dwell time) did not yield consistent results. However, we could estimate t_c rather

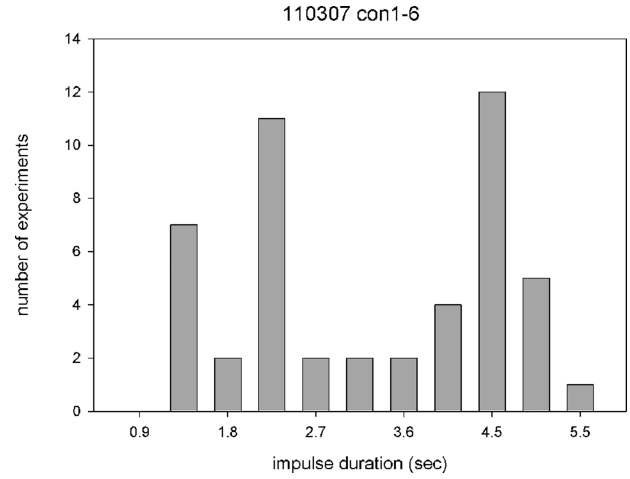

FIGURE 8: The histogram of the times anisotropy of actin was high. The mean duration is defined as $\sum t_s N/\sum N$, where t_s is a given duration and N is the number of measurements with this duration. The total number of experiments was 49. The mean duration was 3.4 s.

accurately. The average frequency during the first 20 s was 0.095 ± 0.015 Hz. The average frequency during the first 20 s using 2 mM ATP was 0.14 ± 0.017. The difference between two means is statistically significant ($t = 5.14$, $P = 2.4 \times 10^{-4}$).

Measuring t_c. It is believed that splitting of one molecule of ATP leads to a single impulse (*14*). In vitro evidence, based on observation of the individual steps of smooth myosin (*6, 7*), myosin V (*8*−*10*), myosin VI (*52, 53*) and kinesin (*54, 55*), suggests that it is indeed so under unloaded conditions (*6, 8, 56, 57*). But this does not necessarily have to be so in isometrically working muscle where a significant external load is applied to cross-bridges and where no gross mechanical work is performed (*58*). Here, splitting of one ATP molecule could lead to multiple mechanical cycles (*59*). Conversely, the energy of hydrolysis could be used for purposes other than performance of mechanical work. Our results suggest that this is indeed the case, because the observed average rate of change of actin orientation was 0.17 Hz, much smaller than myofibrillar ATPase activity. The ATPase activity of our un-cross-linked myofibrils was 89 μmol of Pi/μmol of myosin/min) = 1.5 Hz (labeling with phalloidin or cross-linking did not change ATPase: it was within experimental error of this value). The present results support the idea that the observed rotation of cross-bridges is a result of "slippage", i.e. that cross-bridges that rotate do so only because they are not rigidly held in place. If the conditions were ideally isometric, no rotation would have occurred at all and all the energy of hydrolysis would have been used for maintenance or wasted as heat.

Duty Ratio. The ratio DC = t_s/t_c in isometric contraction was therefore nearly 60%, much larger than measured in vitro (*5, 11*). Under isometric conditions, a cross-bridge acts against maximum load (equal to isometric force), whereas under isotonic conditions it acts initially against a small load. The load increases in time as the muscle is stretched. This is consistent with the fact that isometric force and quick tension recovery seemed to result from two distinctly different molecular processes. Isometric force resulted from a structural change in the actomyosin complex associated with the transition from a weakly bound configuration to a

strongly bound configuration (before the reaction steps in the Huxley−Simmons model), whereas a major component of quick tension recovery originated from transitions among the subsequent strongly bound states (*60*). It is also consistent with the fact that the tension fluctuations were present only in isometrically held actin filaments (*61*), that the sliding distance of the myosin head while it interacts with actin per ATP molecule hydrolyzed decreased with load (*12*), that increasing the stiffness of the optical trap holding actin filament led to shorter duration of actomyosin attachment events (*62*), and that step size may be zero in isometric muscle (*58*).

We considered eight possible artifacts that may have given rise to this observation, and concluded that none is likely:

1. The oscillations are an artifact resulting from spurious sources such as EM CCD readout noise, other instrumental noise, laser instability, air currents on the microscope stage or building vibrations. It is also possible that faster oscillations are missed because the time resolution of the method is too slow to observe fast motions.

This is unlikely, because rigor myofibrils, imaged under identical conditions, showed no oscillations. Time resolution is sufficient, because one frame was collected in 200 ms giving frequency resolution of 5 Hz. Oscillations would have to be much faster than ATPase for the present method to miss them.

2. The oscillations are an artifact resulting from gradients of ATP concentration. This is unlikely, because ours were steady-state experiments, i.e. contraction was initiated by addition of ATP. ATP was added to one side of the experimental chamber, and sucked with a filter paper at the other end. The few minutes necessary to focus was plenty of time to equilibrate the ATP concentration across the chamber. This is the advantage of steady-state experiments, which avoid production of the gradients which could be generated when imposing rapid increase in ATP concentration by rapid photolysis of caged ATP (*63*).

3. The oscillations are an artifact resulting from photobleaching. This is impossible, because the fast Fourier transform was applied either before or after the photobleaching event.

4. The oscillations are an artifact due to movement of myofibrils. It is unlikely that oscillations were due to the change in the number of fluorophores in the 4 × 4 pixel observational area due to shortening of myofibrils. We would have been able to detect shortening of 0.2 μm (limit of resolution) in 100 s, i.e. 2 nm/s. No such shortening occurred in cross-linked myofibrils (see Materials and Methods). But even if it did occur, its frequency would have been negligible: the observational area is 4 × 4 pixels. The back-projected size of a pixel is 16 μm/100 = 160 nm, i.e. linear dimension of ROI is 640 nm. It would take, on average, ~160 s for a single fluorophore to leave this area to give rise to a fluctuation in intensity. Its frequency would have been 0.0006 Hz. When 3 fluorophores were observed, their escape from the area would lead to signal oscillating at 0.02 Hz, much below what was observed. It is also unlikely that oscillations were due to the change in the number of fluorophores in the observational area due to oscillatory motion of myofibrils. Ishiwata et al. found that the myosin II motors show nonlinear auto-oscillation, named SPOC (spontaneous oscillatory contraction). For cardiac muscle it occurred when the activation level was intermediate between those of contraction and relaxation. For skeletal muscle, it required the coexistence of MgATP, MgADP and inorganic phosphate (Pi) at higher pCa (<7) (*64*). In our experiments, however, pCa was fixed at 4.

5. Fluorescence oscillations are an artifact resulting from dissociation of phalloidin from thin filaments. The OFF-rate of UP is slow (see above and ref *43*), but the OFF-rate of RP could, in principle, be faster. Its dissociation−association from actin could have been responsible for oscillations. However, this is unlikely, first because rigor myofibrils did not show any oscillations and second, because if this were the case, it would have been possible to wash out the fluorescent dye with prolonged washing. This has proven impossible: 15 min washing of myofibrils labeled with 1 nM RP + 10 μM UP did not reduce fluorescence at all (in fact, it improved the contrast, probably because the background was reduced). Further, independent measurements of fluorescence correlation spectroscopy (FCS) of contracting myofibrils showed no translational motion of free phalloidin (data not shown).

6. The signal is not reflecting rhodamine concentration, but originates from Trp fluorescence of myofibrils. Even though Trp has practically no absorption at 532 nm, the concentration of RP (0.1 nM) is so much smaller than the concentration of protein (4 μM) that the signal carries a significant contribution from autofluorescence. However, this is impossible, because unlabeled myofibrils had no autofluorescence whatsoever, probably because the sample was only ~100 nm thick.

7. The signal is due to rotation of the edges of the O-bands of contracting muscle because the end of thin filaments may be fluttered or undergo tethered motion sometimes. Such motion does not occur in rigor because the end of thin filament are rigidly fixed by the binding of rigor cross-bridges. This has been checked by FCS. In 9 independent measurements on ~10 molecules in an area near the edge of the I-band, the autocorrelation function was the same in rigor and in contracting myofibrils.

It is unlikely that our observations are due to the fact that the observed actin monomer is too far away from the nearest active cross-bridge to be touched by it. The molar ratio of actin:cross-bridges is ~2:1 (*13*). In isometric contraction only ~1/3 of cross-bridges are active (*26*), so the excess of actin over active heads is about 6. This ratio implies that in ~15% of experiments we can expect to observe a monomer that is near the active cross-bridge. Such actin would be expected to rotate at the ATPase frequency. However, high frequencies were never observed in the total of 19 analyzed experiments. They were also never seen by visual inspection of many more unanalyzed experiments.

8. In relaxed muscle, cross-bridge cycling should stop. We have done 72 experiments on 4 different preparations of myofibrils in rigor, 72 experiments on 4 different preparations in relaxation, and 40 experiments on 4 different preparations during contraction. Myofibrils were labeled with 1 nM RP + 10 μM UP and cross-linked as described to avoid shortening. Sarcomere lengths ranged from 1.73 μm to 2.88 μm. No shortening occurred within 100 s. Rigor myofibrils gave no fluctuations at all. In 56 experiments on relaxed myofibrils we observed no fluctuations at all. In 16 experiments on relaxed myofibrils we observed some fluctuations.

We think that this was due to the fact that some sarcomeres in those 16 myofibrils were not sensitive to Ca^{2+}. If a few troponin or tropomyosin molecules are damaged, than this sarcomere is going to contract even if there is EGTA in bathing solution. All 40 experiments on contracting myofibrils showed fluctuations. In all 40 experiments, the power during the last 20 s was on average 1.7 times smaller than during the first 20 s.

REFERENCES

1. Reedy, M. C. (2000) Visualizing myosin's power stroke in muscle contraction. *J. Cell Sci. 113* (Part 20), 3551–3562.
2. Sweeney, H. L., and Houdusse, A. (2004) The motor mechanism of myosin V: insights for muscle contraction. *Philos. Trans. R. Soc. London, B: Biol. Sci. 359* (1452), 1829–1841.
3. Takagi, Y., Shuman, H., and Goldman, Y. E. (2004) Coupling between phosphate release and force generation in muscle actomyosin. *Philos. Trans. R. Soc. London, B: Biol. Sci. 359* (1452), 1913–1920.
4. Taylor, K. A., Schmitz, H., Reedy, M. C., Goldman, Y. E., Franzini-Armstrong, C., Sasaki, H., Tregear, R. T., Poole, K., Lucaveche, C., Edwards, R. J., Chen, L. F., Winkler, H., and Reedy, M. K. (1999) Tomographic 3D reconstruction of quick-frozen, Ca2+-activated contracting insect flight muscle. *Cell 99* (4), 421–431.
5. Kron, S. J., and Spudich, J. A. (1986) Fluorescent actin filaments move on myosin fixed to a glass surface. *Proc. Natl. Acad. Sci. U.S.A. 83*, 6272–6276.
6. Warshaw, D. M., Hayes, E., Gaffney, D., Lauzon, A. M., Wu, J., Kennedy, G., Trybus, K., Lowey, S., and Berger, C. (1998) Myosin conformational states determined by singlefluorophore polarization. *Proc. Natl. Acad. Sci. U.S.A. 95* (14), 8034–8039.
7. Quinlan, M. E., Forkey, J. N., and Goldman, Y. E. (2005) Orientation of the myosin light chain region by single molecule total internal reflection fluorescence polarization microscopy. *Biophys. J. 89* (2), 1132–1142. Epub 2005 May 13.
8. Forkey, J. N., Quinlan, M. E., Shaw, M. A., Corrie, J. E., and Goldman, Y. E. (2003) Three-dimensional structural dynamics of myosin V by single-molecule fluorescence polarization. *Nature 422* (6930), 399–404.
9. Yildiz, A., Forkey, J. N., McKinney, S. A., Ha, T., Goldman, Y. E., and Selvin, P. R. (2003) Myosin V walks hand-over-hand: single fluorophore imaging with 1.5-nm localization. *Science 300* (5628), 2061–2065. Epub 2003 June 5.
10. Toprak, E., Enderlein, J., Syed, S., McKinney, S. A., Petschek, R. G., Ha, T., Goldman, Y. E., and Selvin, P. R. (2006) Defocused orientation and position imaging (DOPI) of myosin V. *Proc. Natl. Acad. Sci. U.S.A. 103* (17), 6495–6499. Epub 2006 April 13.
11. VanBuren, P. W., Waller, G. S., Harris, D. E., Trybus, K. M., Warshaw, D. M., and Lowey, S. (1994) The essential light chain is required for full force production by skeletal muscle myosin. *Proc. Natl. Acad. Sci. U.S.A. 91*, 12403–12407.
12. Higuchi, H., and Goldman, Y. E. (1995) Sliding distance per ATP molecule hydrolyzed by myosin heads during isotonic shortening of skinned muscle fibers. *Biophys. J. 69* (4), 1491–1507.
13. Bagshaw, C. R. (1982) *Muscle Contraction*, Chapman & Hall, London.
14. Uyeda, T. Q., Kron, S. J., and Spudich, A. A. (1990) Myosin step size. Estimation from slow sliding movement of actin over low densities of heavy meromyosin. *J. Mol. Biol. 214*, 699–710.
15. Harris, D. E., and Warshaw, D. M. (1993) Smooth and skeletal muscle myosin both exhibit low duty cycles at zero load in vitro. *J. Biol. Chem. 268* (20), 14764–14768.
16. Mitsui, T. (1999) Induced potential model of muscular contraction mechanism and myosin molecular structure. *Adv. Biophys. 36*, 107–158.
17. Matsubara, I., Yagi, N., and Hashizume, H. (1975) Use of an X-ray television for diffraction of the frog striated muscle. *Nature 255* (5511), 728–729.
18. Edman, K. A. (1988) Double-hyperbolic force-velocity relation in frog muscle fibres. *J. Physiol. 404*, 301–321.
19. Mitsui, T., and Ohshima, H. (1988) A self-induced translation model of myosin head motion in contracting muscle. I. Force-velocity relation and energy liberation. *J. Muscle Res. Cell Motil. 9* (3), 248–260.
20. Ishijima, A., Harada, Y., Kojima, H., Funatsu, T., Higuchi, H., and Yanagida, T. (1994) Single-molecule analysis of the actomyosin motor using nano-manipulation. *Biochem. Biophys. Res. Commun. 199* (2), 1057–1063.
21. Geeves, M. A., Holmes, K. C., Bodis, E., Szarka, K., Nyitrai, M., Somogyi, B., Razzaq, A., Schmitz, S., Veigel, C., Molloy, J. E., Sparrow, J. C., Furch, M., Fujita-Becker, S., Manstein, D. J., and Cremo, C. R. (2005) The molecular mechanism of muscle contraction. *Adv. Protein Chem. 71* (24), 161–193.
22. Linari, M., Dobbie, I., Reconditi, M., Koubassova, N., Irving, M., Piazzesi, G., and Lombardi, V. (1998) The stiffness of skeletal muscle in isometric contraction and rigor: the fraction of myosin heads bound to actin. *Biophys. J. 74* (5), 2459–2473.
23. Cooke, R., Crowder, M. S., and Thomas, D. D. (1982) Orientation of spin labels attached to cross-bridges in contracting muscle fibres. *Nature 300* (5894), 776–778.
24. Duong, A. M., and Reisler, E. (1989) Binding of myosin to actin in myofibrils during ATP hydrolysis. *Biochemistry 28*, 1307–1313.
25. Berger, C. L., and Thomas, D. D. (1993) Rotational dynamics of actin-bound myosin heads in active myofibrils. *Biochemistry 32* (14), 3812–3821.
26. Cooper, W. C., Chrin, L. R., and Berger, C. L. (2000) Detection of fluorescently labeled actin-bound cross-bridges in actively contracting myofibrils. *Biophys. J. 78* (3), 1449–1457.
27. Thomas, D. D., and Cooke, R. (1980) Orientation of spin-labeled myosin heads in glycerinated muscle fibers. *Biophys. J. 32*, 891–905.
28. Borejdo, J., Assulin, O., Ando, T., and Putnam, S. (1982) Cross-bridge orientation in skeletal muscle measured by linear dichroism of an extrinsic chromophore. *J. Mol. Biol. 158*, 391–414.
29. Shepard, A. A., Dumka, D., Akopova, I., Talent, J., and Borejdo, J. (2004) Simultaneous measurement of rotations of myosin, actin and ADP in contracting skeletal muscle fiber. *J. Muscle Res. Cell Motil. 25*, 549–557.
30. Szczesna, D., and Lehrer, S. S. (1993) The binding of fluorescent phallotoxins to actin in myofibrils. *J. Muscle Res. Cell Motil. 14* (6), 594–597.
31. Bukatina, A. E., Fuchs, F., and Watkins, S. C. (1996) A study on the mechanism of phalloidin-induced tension changes in skinned rabbit psoas muscle fibres. *J. Muscle Res. Cell Motil. 17* (3), 365–371.
32. Prochniewicz-Nakayama, E., Yanagida, T., and Oosawa, F. (1983) Studies on conformation of F-actin in muscle fibers in the relaxed state, rigor, and during contraction using fluorescent phalloidin. *J. Cell Biol. 97*, 1663–1667.
33. Tregear, R. T., and Mendelson, R. A. (1975) Polarization from a helix of fluorophores and its relation to that obtained from muscle. *Biophys. J. 15*, 455–467.
34. Herrmann, C., Sleep, J., Chaussepied, P., Travers, F., and Barman, T. (1993) A structural and kinetic study on myofibrils prevented from shortening by chemical cross-linking. *Biochemistry 32* (28), 7255–7263.
35. Borejdo, J., Muthu, P., Talent, J., Akopova, I., and Burghardt, T. P. (2007) Rotation of actin monomers during isometric contraction of skeletal muscle. *J. Biomed. Optics 12*, 014013.
36. Herrmann, C., Lionne, C., Travers, F., and Barman, T. (1994) Correlation of ActoS1, myofibrillar, and muscle fiber ATPases. *Biochemistry 33* (14), 4148–4154.
37. Lionne, C., Iorga, B., Candau, R., and Travers, F. (2003) Why choose myofibrils to study muscle myosin ATPase? *J. Muscle Res. Cell Motil. 24* (2−3), 139–148.
38. Borejdo, J., Talent, J., Akopova, I., and Burghardt, T. P. (2006) Rotations of a few cross-bridges in muscle by confocal total internal reflection microscopy. *Biochim. Biophys. Acta 1763*, 137–140.
39. Axelrod, D. (1989) Total internal reflection fluorescence microscopy. *Methods Cell Biol. 30*, 245–270.
40. Potma, E. J., van Graas, I. A., and Stienen, G. J. (1994) Effects of pH on myofibrillar ATPase activity in fast and slow skeletal muscle fibers of the rabbit. *Biophys. J. 67* (6), 2404–2410.
41. Matveeva, E., Gryczynski, I., Barnett, A., Leonenko, Z., Lakowicz, J. R., and Gryczynski, Z. (2007) Metal-particle-enhanced fluorescent immunoassays on metal mirrors. *Anal. Biochem. 363*, 239–245.
42. Eggeling, C., Widengren, J., Rigler, R., and Seidel, C. A. M. (1998) Photobleaching of Fluorescent Dyes under Conditions Used for Single-Molecule Detection: Evidence of Two-Step Photolysis. *Anal. Chem. 70*, 2651–2659.

43. De La Cruz, E., and Pollard, T. D. (1994) Transient kinetic analysis of rhodamine phalloidin binding to actin filaments. *Biochemistry 33* (48), 14387–14392.
44. Borejdo, J., and Akopova, I. (2003) Orientational Changes of Cross-Bridges During Single Turnover of ATP. *Biophys. J. 84*, 2450–2459.
45. Borejdo, J., Shepard, A. A., Akopova, I., Grudzinski, W., and Malicka, J. (2004) Rotation of the lever-arm of myosin in contracting skeletal muscle fiber measured by two-photon anisotropy. *Biophys. J. 87*, 3912–3921.
46. Borejdo, J., Gryczynski, Z., Calander, N., Muthu, P., and Gryczynski, I. (2006) Application of Surface Plasmon Coupled Emission to Study of Muscle. *Biophys. J. 91*, 2626–2635.
47. Burghardt, T. P., Charlesworth, J. E., Halsetad, M. F., Tarara, J. E., and Ajtai, K. (2006) In Situ Fluorescent Protein Imaging with Metal Film Enhanced Total Internal Reflection Microscopy. *Biophys. J. 24*, 4662–4671.
48. Burghardt, T. P., Ajtai, K., Chan, D. K., Halstead, M. F., Li, J., and Zheng, Y. (2007) GFP Tagged Regulatory Light Chain Monitors Single Myosin Lever-Arm Orientation in a Muscle Fiber. *Biophys. J. 18*, 2226–2239.
49. Minton, A. P. (1998) Molecular crowding: analysis of effects of high concentrations of inert cosolutes on biochemical equilibria and rates in terms of volume exclusion. *Methods Enzymol. 295*, 127–149.
50. Eisenberg, E., Hill, T. L., and Chen, Y. (1980) Cross-bridge model of muscle contraction. Quantitative analysis. *Biophys. J. 29* (2), 195–227.
51. Baker, J. E., Brosseau, C., Joel, P. B., and Warshaw, D. M. (1992) The biochemical kinetics underlying actin movement generated by one and many skeletal muscle myosin molecules. *Biophys. J. 82* (4), 2134–2147.
52. Park, H., Ramamurthy, B., Travaglia, M., Safer, D., Chen, L. Q., Franzini-Armstrong, C., Selvin, P. R., and Sweeney, H. L. (2006) Full-length myosin VI dimerizes and moves processively along actin filaments upon monomer clustering. *Mol. Cell 21* (3), 331–336.
53. Park, H., Li, A., Chen, L. Q., Houdusse, A., Selvin, P. R., and Sweeney, H. L. (2007) The unique insert at the end of the myosin VI motor is the sole determinant of directionality. *Proc. Natl. Acad. Sci. U.S.A. 104* (3), 778–783. Epub 2007 Jan 9.
54. Quinlan, M. E., Forkey, J. N., and Goldman, Y. E. (2001) Kinesin-ADP: whole lotta shakin' goin' on. *Nat. Struct. Biol. 8* (6), 478–480.
55. Yildiz, A., and Selvin, P. R. (2005) Kinesin: walking, crawling or sliding along? *Trends Cell Biol. 15* (2), 112–120.
56. Lymn, R. W., and Taylor, E. W. (1971) Mechanism of adenosine triphosphate hydrolysis by actomyosin. *Biochemistry 10*, 4617–4624.
57. Houdusse, A., and Sweeney, H. L. (2001) Myosin motors: missing structures and hidden springs. *Curr. Opin. Struct. Biol. 11* (2), 182–194.
58. Worthington, C. R., and Elliott, G. F. (1996) Muscle contraction: the step-size distance and the impulse-time per ATP. *Int. J. Biol. Macromol. 18* (1−2), 123–131.
59. Yanagida, T., and Ishii, Y. (2003) Stochastic processes in nano-biomachines revealed by single molecule detection. *Biosystems 71* (1−2), 233–244.
60. Brenner, B., Chalovich, J. M., and Yu, L. C. (1995) Distinct molecular processes associated with isometric force generation and rapid tension recovery after quick release. *Biophys. J. 68* (4 Suppl.), 106S–111S.
61. Yanagida, T., Ishijima, A., Saito, K., and Harada, Y. (1993) Coupling between ATPase and force-generating attachment-detachment cycles of actomyosin in vitro. *Adv. Exp. Med. Biol. 332*, 339–347.
62. Takagi, Y., Homsher, E. E., Goldman, Y. E., and Shuman, H. (2006) Force generation in single conventional actomyosin complexes under high dynamic load. *Biophys. J. 90* (4), 1295–307. Epub 2005 Dec 2.
63. Borejdo, J., Ushakov, D. S., and Akopova, I. (2002) The essential light chains 1 and 3 rotate differently during muscle contraction. *Biophys. J. 82*, 362a.
64. Ishiwata, S., Shimamoto, Y., Suzuki, M., and Sasaki, D. (2007) Regulation of muscle contraction by Ca2+ and ADP: focusing on the auto-oscillation (SPOC). *Adv. Exp. Med. Biol. 592*, 341–358.

BI7023223